

**Vesicle-micelle transition in aqueous mixtures of the cationic  
dioctadecyldimethylammonium and octadecyltrimethylammonium bromide  
surfactants**

Fernanda Rosa Alves,<sup>1</sup> Maria Elisabete D. Zaniquelli,<sup>2</sup> Watson Loh,<sup>3</sup> Elisabete M.S.  
Castanheira,<sup>4</sup> M. Elisabete C.D. Real Oliveira,<sup>4</sup> and Eloi Feitosa<sup>1,\*</sup>

<sup>1</sup>Physics Department, São Paulo State University, São José do Rio Preto - SP, Brazil

<sup>2</sup>Instituto de Química, Universidade de São Paulo, Ribeirão Preto – SP, Brazil

<sup>3</sup>Instituto de Química, Universidade Estadual de Campinas, Campinas – SP, Brazil

<sup>4</sup>Physics Department, University of Minho, Campus de Gualtar, 4710-057 Braga,  
Portugal

\*To whom correspondence should be addressed:

Eloi Feitosa

Physics Department, IBILCE/UNESP

Rua Cristóvão Colombo, 2265

São José do Rio Preto, SP - Brazil

CEP: 15054-000

Voice: +55 17 3221 22 40

Telefax: +55 17 3221 22 47

e-mail: [eloi@ibilce.unesp.br](mailto:eloi@ibilce.unesp.br)

## Abstract

The vesicle-micelle transition in aqueous mixtures of dioctadecyldimethylammonium and octadecyltrimethylammonium bromide (DODAB and C<sub>18</sub>TAB) cationic surfactants, having respectively double and single chain, was investigated by differential scanning calorimetry (DSC), steady state fluorescence, dynamic light scattering (DLS) and surface tension. The experiments performed at constant up to 1.0 mM total surfactant concentration reveal that these homologue surfactants mix together to form either mixed vesicles and/or micelles, or both of these structures in equilibrium, depending on the relative amount of the surfactants. The main transition melting temperature  $T_m$  of the mixed DODAB-C<sub>18</sub>TAB vesicles is larger than that for the neat DODAB in water owing to the incorporation of C<sub>18</sub>TAB in the vesicle bilayer, however, little amount of C<sub>18</sub>TAB having a minor effect on the  $T_m$  of DODAB. The surface tension decreases sigmoidally with C<sub>18</sub>TAB concentration and the inflection point lies around  $x_{\text{DODAB}} \approx 0.4$ , indicating the onset of micelle formation owing to saturation of DODAB vesicles by C<sub>18</sub>TAB molecules and formation of vesicle structures. At low C<sub>18</sub>TAB concentrations When  $x_{\text{DODAB}} > 0.5$  C<sub>18</sub>TAB molecules are mainly solubilized by the vesicles bilayers, while at high C<sub>18</sub>TAB concentrations but when  $x_{\text{DODAB}} < 0.25$  micelles are dominant. Fluorescence data of the Nile Red probe incorporated in the system at different surfactant molar fractions indicate the formation of micelle and vesicle structures. These structures have apparent hydrodynamic radius  $R_H$  of about 180 and 500-800 nm, respectively, as obtained by DLS measurements.

**Keywords:** DODAB, C<sub>18</sub>TAB, surfactant, DSC, tensiometry, light scattering, melting temperature, Nile Red, steady-state fluorescence.

## Introduction

In aqueous solution surfactants can form a variety of colloidal aggregates and phases depending on the surfactant concentration. When a micelle-forming surfactant is mixed with a vesicle-forming surfactant in aqueous solution, within the range of concentrations that favours the micelle or vesicle formation of the neat surfactants, vesicle-micelle transition occurs, and the intermediate aggregate structures formed in the mixed system depend on the surfactant composition, chemical structure and solvent characteristics. In case these surfactants mix ideally together, the structures of the mixed aggregates are usually investigated in order to elucidate the mechanism of the vesicle-micelle transition.

Cationic vesicles from dioctadecyldimethylammonium bromide (DODAB) in aqueous solution can easily be formed by simply mixing the surfactant molecules in water, followed by warming the mixture to around 60°C, that is, safely above the melting temperature of the surfactant gel to liquid crystalline state transition,  $T_m \approx 43^\circ\text{C}$  [1-6]. The so prepared vesicle dispersions are stable for months even when stored at a temperature below  $T_m$ , for example, at the fridge temperature (5°C). The properties of these vesicles can be mechanically modified by properly sonicating or extruding the dispersion [3], or by adding co-solutes or co-surfactants to the dispersion [4-11]. The  $T_m$  of DODAB in aqueous dispersions can be raised or lowered on addition of co-surfactants [7]; the dependence of DODAB  $T_m$  on the co-surfactant concentration is determined by the nature of the co-surfactant, like the chain length and head group polarity [4-8]. For example, nonionic and zwitterionic surfactants reduce the  $T_m$  of DODAB until complete solubilization of DODAB molecules by the surfactants and the vesicle-micelle transition is complete, and the decrease in  $T_m$  has been ascribed to the formation of “softer” mixed bilayer [4,5]. The surfactant counterion also plays an important role in the thermotropic phase behavior of charged vesicles in general and cationic vesicles in particular. It has been reported that in the absence of inorganic salts like NaBr or NaCl, the  $T_m$  is larger for the chloride homologue (DODAC) than for DODAB, owing to the specific affinity of these counterions to the vesicle interfaces [10]. Furthermore, NaCl rises whereas NaBr lowers the  $T_m$  of DODAB, as reported [9].

Anionic [11,12] and cationic [7,13] surfactants also modify the  $T_m$  of DODAB. Sodium dodecyl sulfate (SDS) yields fusion of DODAB vesicles, while

sodium cholate (NaC) solubilizes DODAB to form micelles that fuse into large aggregates [12]. SDS increases [11] but NaC decreases [12]  $T_m$  of DODAB. Alkyltrimethylammonium salts ( $C_n$ TAB,  $n = 12-18$ ) may reduce, increase or leave constant the  $T_m$  of DODAB, depending on the relative chain length of these surfactants [7,13].

In this communication it is reported that when mixed with DODAB the single chain cationic surfactant octadecyltrimethylammonium bromide ( $C_{18}$ TAB) yields higher  $T_m$  or leave it roughly constant depending on the relative amount of these surfactants. The main  $T_m$  of DODAB increases slightly while a second even higher melting temperature appears at higher  $x_{C_{18}TAB}$ . Furthermore, it is shown the dependence of  $T_m$  on the relative amount of these surfactants. At low concentrations and above the Krafft temperature ( $T_k \approx 38^\circ\text{C}$  in water)  $C_{18}$ TAB self-assembles as globular micelles [14] and in small proportion as bilayer structure, as suggested in this communication. The melting temperature, hydrodynamic radius, surface tension and fluorescence emission of the hydrophobic probe Nile Red, are reported for the DODAB/ $C_{18}$ TAB aqueous mixtures to gain information on the mechanism of association of these surfactants as vesicles or micelles, within the framework of on the vesicle-micelle transition.

## **Experimental**

### Materials

Diocetyltrimethylammonium bromide (DODAB),  $C_{18}$ TAB (octadecyltrimethylammonium bromide) and 9-(diethyl-amino)-5H-benzo[ $\alpha$ ]phenoxazin-5-one (Nile Red) were used as supplied by Aldrich. Ultrapure Milli-Q-Plus water was used in sample preparation. Scheme 1 shows the molecular structures of DODAB,  $C_{18}$ TAB and Nile Red.

### Sample preparation

DODAB and  $C_{18}$ TAB (1.0 mM) aqueous solutions were prepared by weighting the surfactants and warming the dispersion to 60 and 50°C, respectively, that is, safely above the melting ( $T_m \approx 43^\circ\text{C}$ ) [3] and Krafft ( $T_k \approx 38^\circ\text{C}$ ) [14] temperatures of these systems.

Mixed DODAB/C<sub>18</sub>TAB aqueous dispersions were prepared at total surfactant concentration of 0.5 mM for light scattering measurements and 1.0 mM for fluorescence, surface tension and DSC measurements and varying the individual surfactant concentrations. All the experiments were performed at a constant total surfactant concentration and varying the surfactant molar fractions. The data are presented as a function of the surfactant molar fraction, that for DODAB is given by

$$x_{\text{DODAB}} = \frac{[\text{DODAB}]}{[\text{C}_{18}\text{TAB}] + [\text{DODAB}]} \quad (1)$$

where the brackets account for the surfactant molar concentration.

For fluorescence measurements, Nile Red was introduced in the 1.0 mM surfactant systems by injecting 10  $\mu\text{L}$  of a  $10^{-3}$  M stock solution of the probe in ethanol. The final concentration of Nile Red in the solutions is ca 3  $\mu\text{M}$ . The solutions were then cooled to room temperature and left standing for several hours (ca 24 h) to stabilize.

### Fluorescence

Fluorescence measurements were performed using a Spex Fluorolog 2 spectrofluorimeter, equipped with a temperature controlled cuvette holder. Polarized emission spectra were recorded using Glan-Thompson polarizers. All spectra were corrected for the instrumental response of the system.

### Surface Tension ( $\gamma$ )

The surface tension of DODAB/C<sub>18</sub>TAB/water solutions was measured by the drop-volume technique. Drops of the solution were gradually extruded through a capillary and the volume determined to obtain  $\gamma$ , as previously described [2,14,15]. The measurements were made at 40°C to prevent crystal formation.

### Dynamic Light Scattering

Dynamic light scattering (DLS) measurements were made using a Zeta Sizer 3000 HS operating with a laser with power of equipped with 10 mW He-Ne ion laser operating at  $\lambda = 633$  nm was used as light source. From the measured normalized intensity time correlation function, we obtained, through the inverse Laplace transform analysis, the relaxation time distribution, and from the moments of this distribution the diffusion

coefficients of the particles were determined [16]. The apparent hydrodynamic radius was then obtained using the Stokes-Einstein equation

$$R_H = \frac{kT}{6\pi\eta_0 D} \quad (2)$$

where  $D$  is the mean diffusion coefficient,  $k$  is the Boltzmann constant,  $T$  is the absolute temperature and  $\eta_0$  is the solvent viscosity.

### Differential Scanning Calorimetry (DSC)

A VP-DSC (MicroCal, Northampton, MA) calorimeter equipped with 0.542 ml twin cells for the reference and sample solutions was used. The measurements were performed with the scan rate of 1°C/min and temperature range of 5-80°C. The two cells filled with water were run as baseline reference. From the thermograms we obtained  $T_m$ , which is the temperature at the peak maximum, the enthalpy change of this transition, which is proportional to the area under the transition peak, and the transition cooperativity, which is inversely proportional to the peak width. Further Details on the DSC methods and setup can be found elsewhere in previous publications [4-6].

### **Results and discussion**

When  $C_{18}TAB$  (critical micellar concentration,  $CMC \approx 0.35$  mM at 40°C) [17] and DODAB (critical vesicular concentration,  $CVC \approx 0$ ) [2] are mixed together in water, either vesicles or micelles or both can be formed, depending on the surfactant concentration, temperature and ionic strength, since the structure of these surfactant aggregates depends individually on these parameters [9,14]. In this communication, it is reported the effect of the surfactant concentration and temperature on some physical properties of the DODAB/ $C_{18}TAB$ /water system.

Above CMC and at room temperature (ca 25°C), neat  $C_{18}TAB$  in water precipitates as hydrated crystals (HC) within ca. 24 hours of preparation, since the system is below the Krafft temperature ( $T_k \approx 38^\circ\text{C}$ . [14] of this surfactant in water. DODAB, on the other hand, has quite low CVC [2] and is poorly soluble in water below  $T_m \approx 43^\circ\text{C}$ . Above this critical temperature DODAB forms large unilamellar vesicles (LUV) at concentrations up to ca 1 mM [1-13].

In presence of up to ca  $x_{\text{DODAB}} = 0.25$  ( $x_{\text{C}_{18}\text{TAB}} > 0.75$ ) the dispersion is rich in  $\text{C}_{18}\text{TAB}$  micelles and there are some HC precipitates at 25°C in equilibrium with mixed vesicles; above  $x_{\text{DODAB}} \approx 0.25$  this DODAB concentration the dispersion is bluish and rich in vesicle structures, and most of the  $\text{C}_{18}\text{TAB}$  molecules are either incorporated in the vesicle bilayers or free in solution as monomers. The phase diagram for the DODAB/ $\text{C}_{18}\text{TAB}$ /water system for 1.0 mM total surfactant concentration and 25°C is shown in the supporting materials (Fig. SM1). It indicates the region of vesicle dispersion ( $L_1$ ),  $x_{\text{DODAB}} > 0.25$  and that of crystal precipitates in vesicle dispersion ( $L_1 + \text{HC}$ ),  $x_{\text{DODAB}} < 0.25$ . Most probably the unbound  $\text{C}_{18}\text{TAB}$  surfactants to the vesicle structures precipitate as hydrated crystals. The phase diagram was constructed by preparing a number of samples having different compositions that were kept standing for months at 25°C before the phase border being defined. The samples were observed by naked eyes and the properties of surfactant mixtures at varying surfactant concentration were monitored by a number of techniques, as discussed below. For all experimental data the error does not exceed 5%.

### Surface Tension results

The surface tension ( $\gamma$ ) data for the DODAB/ $\text{C}_{18}\text{TAB}$ /water system were collected at 40°C (slightly above  $T_k$  of neat  $\text{C}_{18}\text{TAB}$  in water and below  $T_m$  the of neat DODAB in water) and constant 1.0 mM total surfactant concentration (Fig. 1). For  $x_{\text{DODAB}} = 1$  (neat DODAB in water)  $\gamma$  approaches that of pure water (ca 72.0 mNm<sup>-1</sup>), owing to the very low CVC of DODAB in water [2]. In presence of up to  $x_{\text{C}_{18}\text{TAB}} \approx 0.5$  ( $x_{\text{DODAB}} > 0.5$ ), there is no significant decrease change in  $\gamma$ , indicating that  $\text{C}_{18}\text{TAB}$  is solubilized into the vesicle bilayer to form mixed DODAB- $\text{C}_{18}\text{TAB}$  vesicles instead of adsorbing at the air/water interface. At higher  $\text{C}_{18}\text{TAB}$  content, however,  $\gamma$  decreases sigmoidally, with the inflection point around  $x_{\text{DODAB}} \approx 0.4$ , to attain the minimum value of ca 36 mNm<sup>-1</sup>, that is comparable similar to the value of neat  $\text{C}_{18}\text{TAB}$  in water above CMC [14]. The decrease in  $\gamma$  is most probably due to saturation of the vesicle bilayer by  $\text{C}_{18}\text{TAB}$  and the excess surfactant monomers that remain free in solution act at the air-water interface of the system. For  $x_{\text{DODAB}} < 0.25$  the solution is dominated by  $\text{C}_{18}\text{TAB}$ -DODAB mixed micelles. Finally, neat  $\text{C}_{18}\text{TAB}$  (1.0 mM) in water assembles mainly as globular micelles, as reported [14].

### Dynamic light scattering (DLS) results

DLS data were collected at 25°C and constant 0.5 mM total surfactant concentration, and the mean apparent hydrodynamic radius ( $R_H$ ) of the aggregates monitored as a function of  $x_{\text{DODAB}}$  the surfactant molar fraction (Fig. 2). At higher concentrations DODAB vesicles scatter too much light, thus being not suitable for the data analyses [1]. Accordingly, for the neat DODAB vesicles  $R_H \approx 544$  nm and in presence of increasing amount of C<sub>18</sub>TAB (decreasing  $x_{\text{DODAB}}$ )  $R_H$  tends to increase to a maximum value of  $R_H \approx 820$  nm when  $x_{\text{DODAB}} \approx 0.3$ , and then it decreases to the value of  $R_H$  for the neat C<sub>18</sub>TAB micelles,  $R_H \approx 180$  nm. The large micelle size has to do with the trend of C<sub>18</sub>TAB not to assemble as globular micelles, as reported [14].

The vesicle growth may be attributed to the incorporation of C<sub>18</sub>TAB into the DODAB bilayer to favor larger vesicle formation. The  $R_H$  maximum at  $x_{\text{DODAB}} \approx 0.3$  corresponds to the onset of micelle formation. Beyond this point ( $x_{\text{DODAB}} < 0.3$ ),  $R_H$  decreases to attain the value of the neat C<sub>18</sub>TAB micelles. The decrease in  $R_H$  is most probably related to the formation of increasing amount of mixed micelles in equilibrium with a decreasing amount of mixed DODAB vesicles. Since the micelles are smaller than the vesicles, the mean size reported might be the average size of the vesicle and micelle populations.



### Differential scanning calorimetry (DSC) results

The DSC traces for 1.0 mM total surfactant concentration in mixed DODAB/C<sub>18</sub>TAB aqueous dispersions are shown in Fig. 3 for varying surfactant concentrations. The melting temperature,  $T_m$ , melting enthalpy ( $\Delta H$ ) and peak width ( $\Delta T_{1/2}$ ) related to the main transition are also shown in Figs. 4 and 5 and Table SM1, as function of  $x_{\text{DODAB}}$ . Accordingly, the neat DODAB/water dispersion ( $x_{\text{DODAB}} = 1$ ) exhibits a small pre-transition peak around  $T_s = 33.3^\circ\text{C}$ , in addition to the main transition at  $T_m = 42.5^\circ\text{C}$ , as reported before [3]. The pre- and main transitions are related to the transitions from the gel phase to the rippled gel phase and from this to the liquid-crystalline (LC) phase, respectively, upon raising the temperature [18,19]. Since the pre-transition vanishes in presence of a small amount of C<sub>18</sub>TAB (Fig.3), mixed C<sub>18</sub>TAB-DODAB vesicles exhibit a direct gel-LC phase transition.

Even though the vesicle dispersions are quite polydisperse [1,2], the width of the main transition peak is rather narrow [3], thus indicating a little dependence of  $T_m$  on the vesicle curvature and structure (like multilamellar or multistructural) in dispersions of large vesicles, and does not change with surfactant concentration except for the intermediate range of  $x_{\text{DODAB}} = 0.5-0.9$  where there is some peak overlapping, indicating that C<sub>18</sub>TAB is solubilized in different vesicle populations, according to the two-population model for the vesicle dispersions of DODAB [1]. In this range of concentration the large values of  $\Delta T_{1/2}$  (Fig. 5) are meaningless since they are related to peak overlapping instead of single transition peaks.

The peak related to the main transition for neat DODAB in water is slightly shifted upward, that is,  $T_m$  increases just a little bit slightly on increasing  $x_{\text{C}_{18}\text{TAB}}$  up to ca 0.7 wt%, when the relative amount of C<sub>18</sub>TAB, whereas a new peak appears at a slightly higher temperature overlapping the main transition peak. By further increasing the amount of C<sub>18</sub>TAB, the intensity of the neat DODAB main peak decreases while the intensity of the additional peak becomes more pronounced. Finally, the main peak for the DODAB-rich vesicles disappears around ca  $x_{\text{DODAB}} \approx 0.5$  (Fig. 3), indicating the presence of mixed vesicles dominated by C<sub>18</sub>TAB that exhibit higher  $T_m$ .

The presence of two main transitions associated to the main peak can be explained by the presence of two populations of vesicles in the neat DODAB aqueous

dispersion that differ mainly in size and structure (multilamellar vs. multistructural) [1] and also to the different surfactant packing of DODAB and C<sub>18</sub>TAB which determines the vesicle curvature. Since T<sub>m</sub> tends to increase with vesicle size [3], the lower and higher temperature main peaks may be related to the higher- and lower-curvatures vesicles, respectively. Since C<sub>18</sub>TAB yields vesicle growth (Fig. 2), the population of smaller vesicles may be reduced in comparison with the larger ones. Thus, as the relative concentration of C<sub>18</sub>TAB increases, the peak intensity for the C<sub>18</sub>TAB-rich vesicles increases, while the one for DODAB-rich vesicles decreases to disappear around the equimolar concentration of the surfactants.

Up to  $x_{\text{C}_{18}\text{TAB}} \approx 0.3$  ( $x_{\text{DODAB}} \geq 0.7$ ), T<sub>m</sub> is roughly the same (or slightly higher), (Fig. 4) thus indicating that the C<sub>18</sub>TAB monomers are incorporated into the DODAB vesicles to form mixed DODAB-C<sub>18</sub>TAB vesicles with the C<sub>18</sub>TAB monomers distributed homogeneously within the DODAB bilayer, such that the mixed vesicles exhibit similar characteristics to the neat DODAB vesicles. For  $x_{\text{DODAB}}$  lower than 0.7, there is a pronounced increase in T<sub>m</sub> until  $x_{\text{DODAB}}$  approaches 0.3, when T<sub>m</sub>  $\approx$  47°C and mixed DODAB-C<sub>18</sub>TAB micelles are formed. In fact the higher T<sub>m</sub> comes from a second peak in the thermogram that initially overlap with the original peak, and these two peaks may be due to solubilization of C<sub>18</sub>TAB in different vesicle populations. When the amount of C<sub>18</sub>TAB is further increased, T<sub>m</sub> remains roughly constant, indicating that the C<sub>18</sub>TAB monomers are not solubilized anymore by the (saturated) vesicle bilayers.

Fig. 3 insert indicates a rather broad peak at T<sub>k</sub>'  $\approx$  26.7°C for neat C<sub>18</sub>TAB in water. This critical temperature is lower than that expected for the Krafft point of this system (ca 38°C) [14] and may be related to a transition in the micelle structure, since at this concentration and temperature the rate of crystal formation is much slower than the DSC scan rate. In presence of small amount of DODAB T<sub>k</sub>' increases but the peak intensity decreases to vanish around  $x_{\text{DODAB}} \approx 0.8$ . The sharper peak above 40°C comes from the main transition.

Interestingly C<sub>18</sub>TAB exhibits in addition to the peak at T<sub>k</sub>' = 26.7°C, an additional peak centered at T<sub>m</sub> = 46°C. Neither these peaks have to do with the Krafft phenomenon that takes place for this surfactant around 40°C [2]. Even though the origin for these peaks is not clear, the smaller one centered at T<sub>m</sub> = 46°C is most probably related to the trend of C<sub>18</sub>TAB to form bilayer-like structures, as reported [14]. Upon addition of DODAB, the peak at T<sub>m</sub> increases intensity whereas the one at

$T_k'$  is inhibited. According to Fig. 4  $T_m$  initially increases to a maximum plateau around 47°C and then it decreases to values comparable to that of neat DODAB, meaning that the vesicle bilayers dominated by  $C_{18}TAB$  are more compact than those dominated by DODAB.

The melting enthalpy decreases monotonically with the amount of  $C_{18}TAB$  concentration (Fig. 5), also indicating that the  $C_{18}TAB$ -rich bilayer is more densely packed relative to that of DODAB. Figure 5 also shows the effect of  $x_{DODAB}$  on the width  $\Delta T_{1/2}$  of the main transition peak. The larger  $\Delta T_{1/2}$  for  $x_{DODAB} \approx 0.5-0.9$  is due to the overlap of the two main peaks that might be related to the two populations of DODAB vesicles present in solution that mainly differ by the relative fraction of  $C_{18}TAB$  solubilized into the vesicle bilayers. Except for the region of peak overlap, the width of all single peaks is rather narrow, indicating high cooperativity of the main transition. In fact the peaks are narrower for the  $C_{18}TAB$ -rich than for the DODAB-rich vesicles.

### Fluorescence results

The fluorescence probe Nile Red (NR) has been extensively used as a probe for lipid aggregates, such as vesicles, due to its hydrophobic nature that allow it to be incorporated in the bilayer moiety [20-23]. In addition, this probe exhibits a solvatochromic behavior and in polar media it is observed a red shift in the emission maximum, together with fluorescence quenching, due to the capability of NR to establish hydrogen bonds with protic solvents [24]. As a consequence, the NR emission in water is very weak with  $\lambda_{max} \approx 660$  nm [25].

Figure 6 shows the emission spectra of NR incorporated in the DODAB/ $C_{18}TAB$ /water system at 25°C, for selected surfactant molar fractions. The fluorescence intensity increases when  $x_{DODAB}$  decreases ( $x_{C_{18}TAB}$  increases). The lower fluorescence emission for the neat DODAB/water system ( $x_{DODAB} = 1$ ) indicates that NR feels a water-rich environment in DODAB vesicles. In fact, the maximum emission wavelength for  $x_{DODAB} = 1$ ,  $\lambda_{max} \approx 650$  nm, is close to the value for pure water ( $\lambda_{max} \approx 660$  nm) [25], probably due to the fact that at room temperature (below  $T_m = 42.5^\circ C$ ) DODAB vesicle bilayers are in the gel phase, thus hindering the probe to penetrate deeper in the lipid bilayer.

When  $x_{\text{DODAB}}$  decreases, the emission intensity increases monotonically (Fig. 6), indicating that NR becomes less exposed to water in the mixed aggregates. This can be explained by the formation of larger structures with a lower curvature, due to the incorporation of  $\text{C}_{18}\text{TAB}$  into the DODAB bilayer, as shown by the light scattering data (Fig. 2). At higher  $\text{C}_{18}\text{TAB}$  content ( $x_{\text{DODAB}} < 0.3$ ), the further increase in NR fluorescence intensity may be justified by the formation of an increasing amount of mixed micelles, where NR feels a more fluid (less viscous) environment and may achieve a deeper penetration.

The variation of the maximum emission wavelength ( $\lambda_{\text{max}}$ ) of NR with increasing  $x_{\text{DODAB}}$  (Fig. 6 insert) indicates the same trend. At 25°C (below  $T_m$ ), in the gel phase,  $\lambda_{\text{max}}$  decreases with decreasing  $x_{\text{DODAB}}$ , thus indicating an increasing hydrophobicity of the local environment of NR when the relative amount of  $\text{C}_{18}\text{TAB}$  is increased. An opposite behavior of  $\lambda_{\text{max}}$  is observed at 55°C (above  $T_m$ ), in the liquid-crystalline phase, where NR feels a more hydrophobic environment at higher  $x_{\text{DODAB}}$ . These results indicate that the aggregate bilayer fluidity depends both on temperature and surfactant composition, and plays an important role in the probe location in the mixed systems.

Figure 7 shows the average steady-state fluorescence anisotropy,  $r$ , of NR in DODAB/ $\text{C}_{18}\text{TAB}$ /water mixtures, obtained at increasing temperature, for  $x_{\text{DODAB}}$  varying from 0 to 1. The anisotropy is given by

$$r = \frac{I_{\text{VV}} - G I_{\text{VH}}}{I_{\text{VV}} + 2G I_{\text{VH}}} \quad (3)$$

where  $I_{\text{VV}}$  and  $I_{\text{VH}}$  are the intensity of the emission spectra obtained with vertical and horizontal polarization, respectively (for vertically polarized excitation light), and  $G = I_{\text{HV}}/I_{\text{HH}}$  is the instrument correction factor, where  $I_{\text{HV}}$  and  $I_{\text{HH}}$  are the emission intensities obtained with vertical and horizontal polarization (for horizontally polarized excitation light).

A high steady-state fluorescence anisotropy value is related to a low degree of rotation of the fluorescence probe. Therefore, anisotropy variations are indicative of changes in fluidity of the probe environment. When temperature increases above  $T_m$ , a decrease in anisotropy is observed resulting from the decrease in the medium viscosity in the liquid-crystalline phase.

For neat DODAB vesicles ( $x_{\text{DODAB}} = 1$ ) the anisotropy is high at temperatures below  $T_m$ , in the gel phase, and exhibits a pronounced decrease upon the gel to liquid-crystalline transition, as previously observed [6]. For the mixed surfactant systems and temperature below 35°C, the anisotropy decreases monotonically with the decrease in the DODAB content, indicating an average increase in fluidity of the mixed aggregates.

In the liquid crystalline phase the anisotropy of the mixed systems for  $x_{\text{DODAB}} > 0.3$  is similar to the value obtained for neat DODAB vesicles. However, a different behaviour was observed for  $x_{\text{DODAB}} \leq 0.3$ , where the anisotropy approaches the value for neat C<sub>18</sub>TAB in water. This indicates that for ca  $x_{\text{DODAB}} > 0.3$ , the aggregates are dominated by mixed vesicles, while for lower  $x_{\text{DODAB}}$ , the aggregates are dominated by mixed micelles. This is supported by the surface tension data that approach the value for the neat DODAB/water system when  $x_{\text{DODAB}} > 0.5$  (Fig. 1). Since the CMC of C<sub>18</sub>TAB in water at 40°C is ca 0.35 mM [17], it is possible that some mixed micelles and vesicles co-exist when  $x_{\text{DODAB}} < 0.5$ . This could explain the strong attenuation of the phase transition in the anisotropy plots for  $x_{\text{DODAB}} = 0.4$  and 0.5 (Fig. 7).

Figure 8 shows the variation of the total fluorescence intensity,  $I_{\text{total}} = I_{\text{VV}} + 2GI_{\text{VH}}$ , with temperature for three different DODAB molar fractions (for other values of  $x_{\text{DODAB}}$  similar data were obtained – results not shown). In the mixed surfactant systems, a maximum is observed around 47°C, close to  $T_m$ . Below this temperature, in the gel phase, it can be observed a slight increase in fluorescence intensity followed by a steep rise around  $T_m$ . This may be due to an increase in bilayer fluidity (chain melting) of the system, causing a deeper penetration of NR in the mixed aggregates. This behavior exceeds the usual fluorescence quenching with temperature, due to the increase in the competitive non-radiative processes, as observed for the neat C<sub>18</sub>TAB system ( $x_{\text{DODAB}} = 0$ ). Above DODAB  $T_m$ , in the liquid-crystalline phase, the emission intensity decreases with increasing temperature, which is the usual behavior.

The less abrupt increase in  $I_{\text{total}}$  for  $x_{\text{DODAB}} = 0.3$  relative to  $x_{\text{DODAB}} = 0.7$  may reflect the lower transition temperature for the latter molar fraction (Fig. 4 and Table SM1). However, the fluorescence measurements are not sensitive enough to small variations in  $T_m$  as observed by DSC.

## Conclusions

Based in the present results of differential scanning calorimetry, dynamic light scattering, NR fluorescence and tensiometry the following conclusions can be outlined: At 1 mM DODAB and C<sub>18</sub>TAB form vesicles and micelles, respectively. By mixing these surfactants mixed vesicles and/or micelles are formed. The melting temperature ( $T_m$ ) for the mixed vesicles is higher than that for neat DODAB, so as the hydrodynamic radii for the mixed micelles and mixed vesicles. In the gel phase the average fluidity of the aggregates increases with the increasing amount of C<sub>18</sub>TAB, while in the liquid-crystalline phase two regions are distinguished, one with the presence of vesicle structures ( $x_{\text{DODAB}} > 0.3$ ) and the other dominated by higher fluid mixed micelles.

Association colloids with well defined and controlled properties, such as melting temperature, size and polydispersity, can thus be formed by mixing surfactants aiming the development of structures that contain domains of solubilization for specific solute molecules for different applications.

## Acknowledgements

FRA and EF thank CNPq for PhD and research grant (Grant 304543/2006-3), respectively. EF also thanks FAPESP for supporting his visit to Universidade do Minho (Grant 07/51039-3). EMSC and MECDRO thanks FCT-Portugal for funding through Centro de Física of Universidade do Minho.

## References

- [1] E. Feitosa, G. Karlsson, K. Edwards, *Chem. Phys. Lipids* 140 (2006) 66.
- [2] E. Feitosa, W. Brown, *Langmuir* 13 (1997) 4810.
- [3] E. Feitosa, P.C.A. Barreleiro, G. Olofsson, *Chem. Phys. Lipids* 105 (2000) 201.
- [4] P.C.A. Barreleiro, G. Olofsson, N.M. Bonassi, E. Feitosa, *Langmuir* 18 (2002) 1024.
- [5] E. Feitosa, N.M. Bonassi, W. Loh, *Langmuir* 22 (2006) 4512.

- [6] E. Feitosa, F.R. Alves, A. Niemiec, M.E.C.D. Real Oliveira, E.M.S. Castanheira, A.L.F. Baptista, *Langmuir* 22 (2006) 3579.
- [7] A. Kacperska, *J. Thermoch. Analysis* 45 (1995) 703.
- [8] M.J. Blandamer, B. Briggs, M.D. Butt, P.M. Cullis, M. Waters, J.B.F.N. Engberts, D. Hoekstra, *J. Chem. Soc. Faraday Trans.* 90 (1994) 727.
- [9] E. Feitosa, P.C.A. Barreleiro, *Prog. Coll. Polym. Sci.* 128 (2004) 163.
- [10] C.R. Benatti, E. Feitosa, R.M. Fernandez, M.T. Lamy-Freund, *Chem. Phys. Lipids* 111 (2001) 93.
- [11] J. Cocquyt, U. Olsson, G. Olofsson, P. Van der Meeren, *Langmuir* 20 (2004) 3906.
- [12] F.R. Alves, E. Feitosa, *Thermochim. Acta* 450 (2006) 76.
- [13] M.J. Blandamer, B. Briggs, P.M. Cullis, A. Kacperska, J.B.F.N. Engberts, D. Hoekstra, *J. Indian Chem. Soc.* 70 (1993) 347.
- [14] M. Swanson-Vethamuthu, E. Feitosa, W. Brown, *Langmuir* 14 (1998) 1590.
- [15] E. Tornberg, *J. Coll. Interf. Sci.* 60 (1977) 50.
- [16] W. Brown, *Dynamic Light Scattering. The Method and Some Applications.* Clarendon Press, Oxford, 1993.
- [17] J. Mata, D. Varade, P. Bahadur, *Thermochimica Acta* 428 (2005) 147.
- [18] P.L. Luisi, B.E. Straub, in *Reverse Micelles – Biological and Technological Relevance of Amphiphilic Structures in Apolar Media.* Plenum Press, New York and London, 1984.
- [19] D.F. Evans, H. Wennerström, *The Colloidal Domain.* Wiley-VCH, 1994.
- [20] P. Greenspan, S.D.J. Fowler, *Lipid Res.* 26 (1985) 781.
- [21] I. Krishnamoorthy, G. Krishnamoorthy, *J. Phys. Chem. B* 15 (2001) 1484.
- [22] P.J.G. Coutinho, E.M.S. Castanheira, M.C. Rei, M.E.C.D. Real Oliveira, *J. Phys. Chem. B* 106 (2002) 12841.
- [23] G. Hungerford, E.M.S. Castanheira, A.L.F. Baptista, P.J.G. Coutinho, M.E.C.D. Real Oliveira, *J. Fluorescence* 15 (2005) 835.
- [24] A. Cser, K. Nagy, L. Biczók, *Chem. Phys. Lett.* 360 (2002) 473.

- [25] G. Hungerford, E.M.S. Castanheira, M.E.C.D. Real Oliveira, M.G. Miguel, H.D. Burrows, *J. Phys. Chem. B* 106 (2002) 4061.



## Figure texts

**Fig. 1** – The effect of DODAB (or C<sub>18</sub>TAB) molar fraction on the surface tension of water-air interface for the DODAB/C<sub>18</sub>TAB/water system. The total surfactant concentration is 1.0 mM and data obtained at 40°C. It indicates regions dominated by micelles (I), micelles and vesicles (II) and vesicles (III). Ves = vesicle, Mic = micelle, Surf = surfactant.

**Fig. 2** – The effect of DODAB (or C<sub>18</sub>TAB) molar fraction on the apparent hydrodynamic radius (R<sub>H</sub>) of the surfactant aggregates in the DODAB/C<sub>18</sub>TAB/water system, at the total surfactant concentration of 0.5 mM (25°C). The dashed line is just a guide for the eyes.

**Fig. 3** – DSC upscan thermograms for the mixture DODAB/C<sub>18</sub>TAB/water, for 1.0 mM total surfactant concentration and varying DODAB molar fraction (numbers beside the curves). Insert shows the expanded thermograms for neat C<sub>18</sub>TAB in water and for  $x_{\text{DODAB}} = 0, 0.1$  and  $0.2$ .

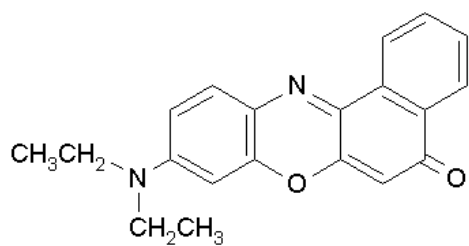
**Fig. 4** – The effect of DODAB (or C<sub>18</sub>TAB) molar fraction on the melting temperature (T<sub>m</sub>) of the cationic mixed DODAB/C<sub>18</sub>TAB aqueous dispersions.

**Fig. 5** – The effect of DODAB (or C<sub>18</sub>TAB) molar fraction on the enthalpy change ( $\Delta H$ ) width of the melting peak ( $\Delta T_{1/2}$ ) for the cationic mixed DODAB/C<sub>18</sub>TAB aqueous dispersions.

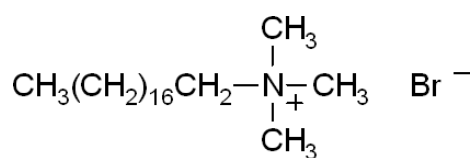
**Fig. 6** – Fluorescence spectra of Nile Red in DODAB/C<sub>18</sub>TAB/water mixed systems for several  $x_{\text{DODAB}}$  at 25°C ( $\lambda_{\text{exc}} = 550$  nm). Insert: Maximum emission wavelength of Nile Red in DODAB/C<sub>18</sub>TAB/water mixed systems in water, below (T = 25°C) and above (T = 55°C) the melting temperature, as a function of  $x_{\text{DODAB}}$ .

**Fig. 7** – Steady-state anisotropy of Nile Red in DODAB/C<sub>18</sub>TAB/water mixed systems for selected DODAB molar fractions.

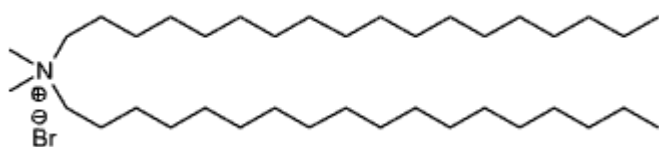
**Fig. 8** – Total intensity of fluorescence ( $I_{\text{total}} = I_{\text{VV}} + 2GI_{\text{VH}}$ ) of Nile Red in DODAB/C<sub>18</sub>TAB/water mixed systems for selected DODAB molar fractions.



**Nile Red**



**C<sub>18</sub>TAB**



**DODAB**

**Scheme 1** – Molecular structures of Nile Red, C<sub>18</sub>TAB and DODAB.

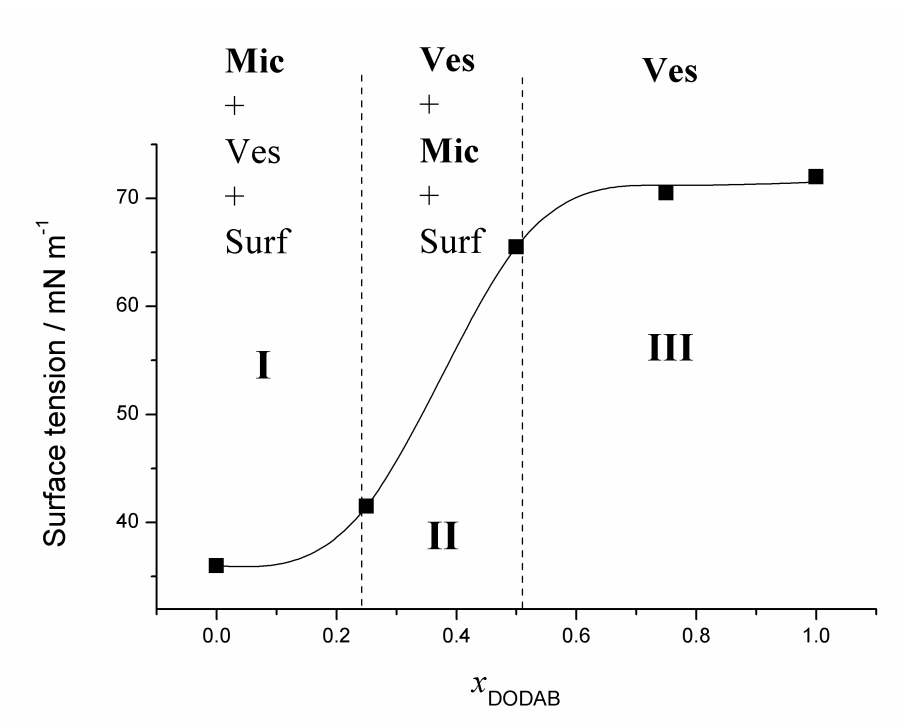


**Fig. 1,** Alves *et al.*

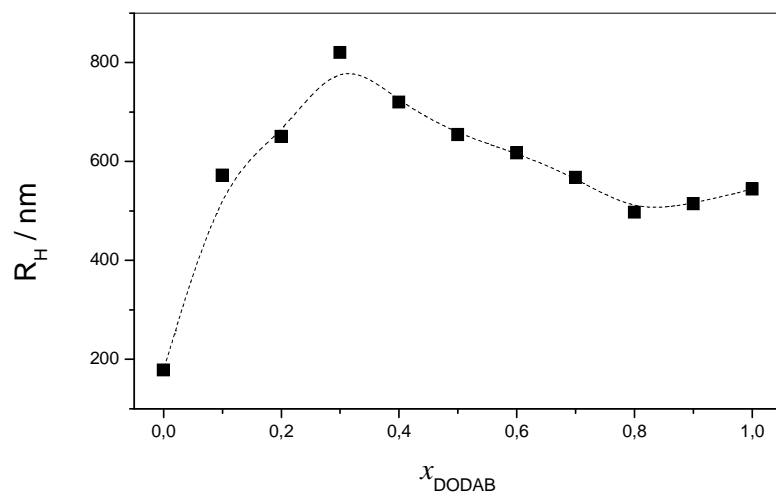


**Fig. 2,** Alves *et al.*

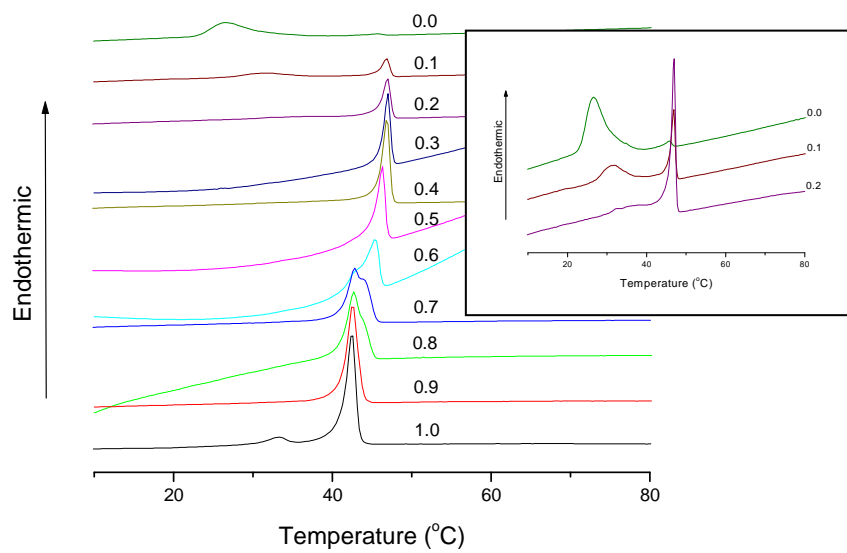


**Fig. 3,** Alves *et al.*

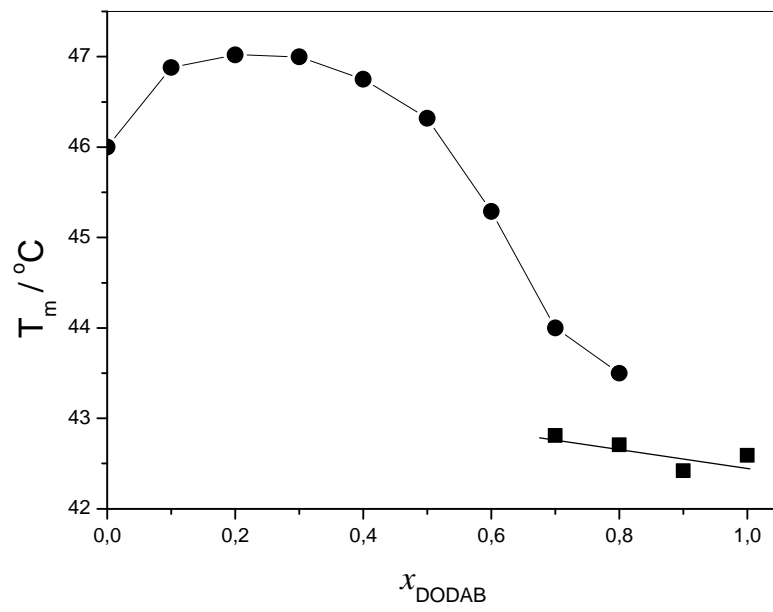


**Fig. 4,** Alves *et al.*

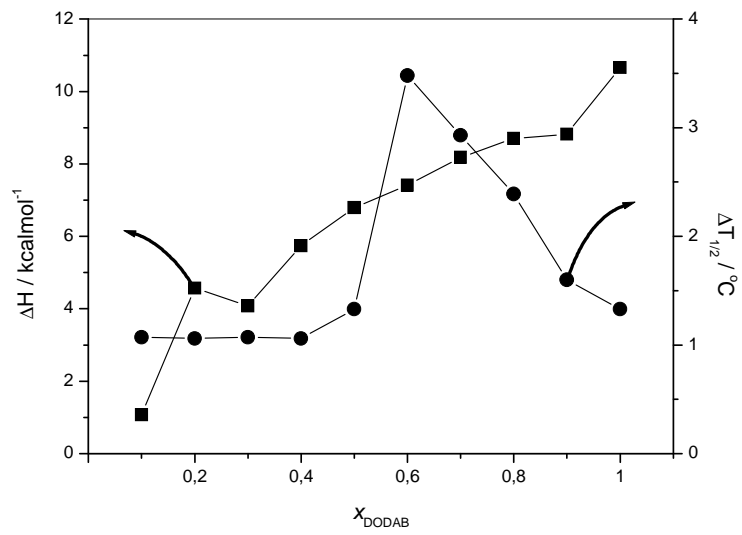


**Fig. 5,** Alves *et al.*



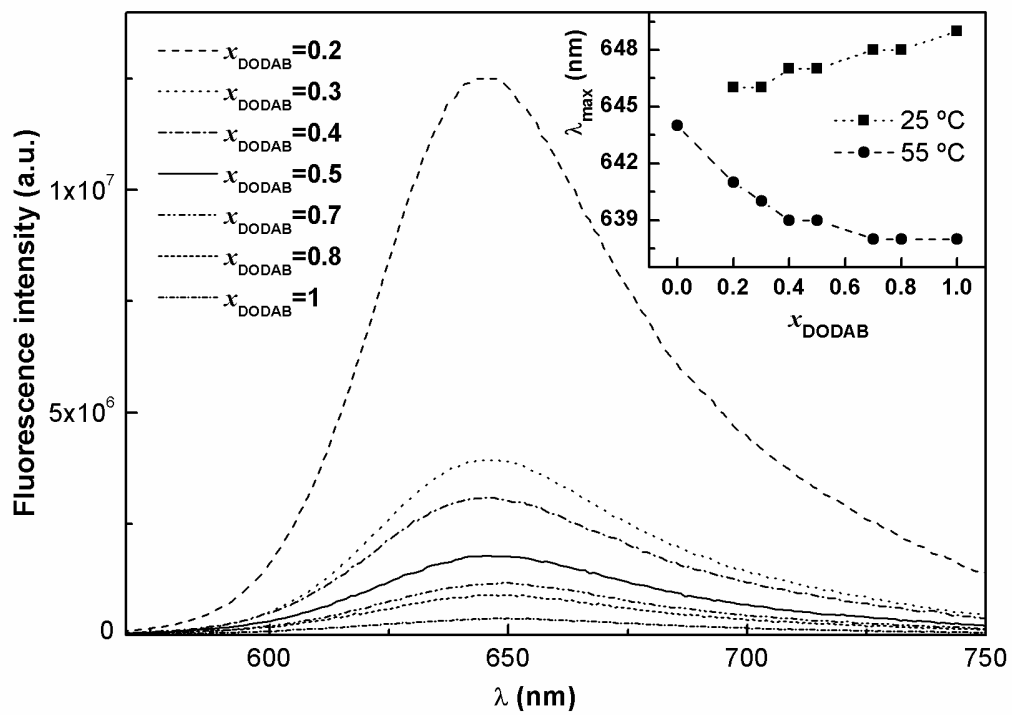


**Fig. 6,** Alves *et al.*

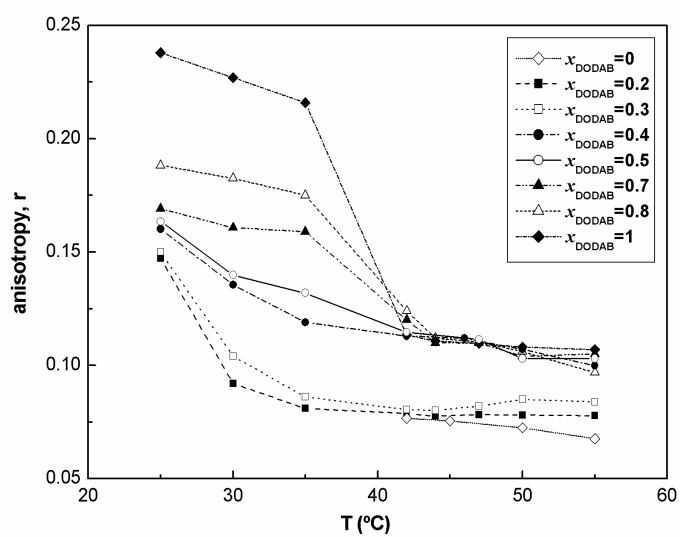


**Fig. 7,** Alves *et al.*

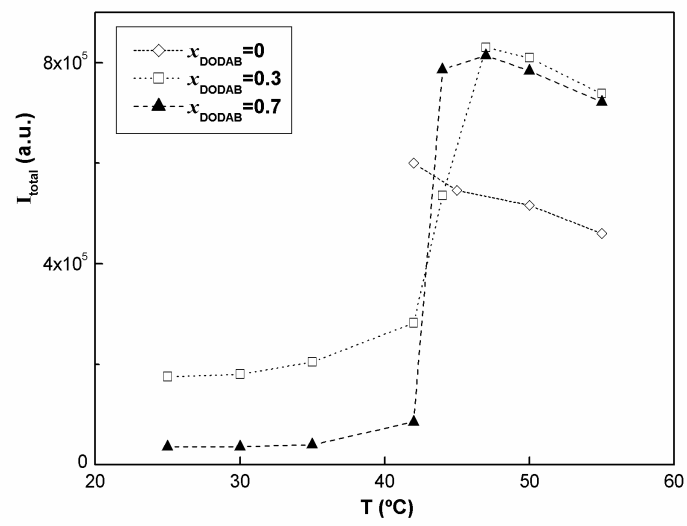
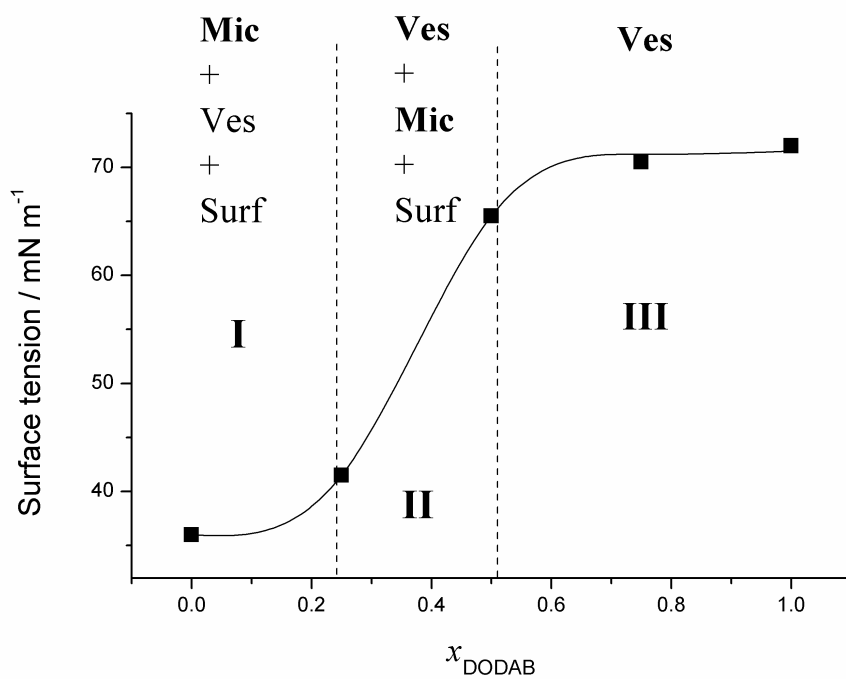


**Fig. 8,** Alves *et al.*



## Graphical Abstract



### Vesicle-micelle transition in aqueous mixtures of the cationic dioctadecyldimethylammonium and octadecyltrimethylammonium bromide surfactants

Fernanda Rosa Alves, Maria Elisabete D. Zaniquelli, Watson Loh, Elisabete M.S. Castanheira, M. Elisabete C.D. Real Oliveira, and Eloi Feitosa

**Supporting materials** for JCIS-07-1096

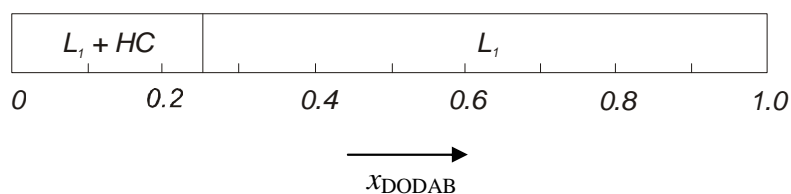


**Fig. SM1** – Phase diagram for the DODAB/C<sub>18</sub>TAB/water system, at 1.0 mM total surfactant concentration and varying the individual surfactant molar fraction. Similar diagram was obtained for 0.5 mM total surfactant concentration (not shown). L<sub>1</sub> and HC account for vesicle phase and hydrated crystals, respectively.

**Table SM1:** Main and pre-transition temperatures, enthalpy and width of the melting transition peak for different DODAB molar fractions. T<sub>k</sub>' accounts either for DODAB pre-transition temperature or neat C<sub>18</sub>TAB/water structure transition. For  $x_{\text{DODAB}} = 0.7$  and 0.8 there are two values of T<sub>m</sub> due to the overlapping of the peaks.

| $x_{\text{DODAB}}$ | T <sub>m</sub> (°C) | T <sub>s</sub> or T <sub>k</sub> ' (°C) | ΔH (kcal mol <sup>-1</sup> ) | ΔT <sub>1/2</sub> (°C) |
|--------------------|---------------------|---|------------------------------|------------------------|
| 1.0                | 42.59               | 33.3                                    | 9.74                         | 1.33                   |
| 0.9                | 42.42               | 32.5                                    | 9.57                         | 1.60                   |
| 0.8                | 42.71<br>(43.5)     | ---                                     | 7.71                         | 2.39                   |
| 0.7                | 42.81<br>(44.0)     | ---                                     | 7.85                         | 2.93                   |
| 0.6                | 45.29               | ---                                     | 8.65                         | 3.48                   |
| 0.5                | 46.32               | ---                                     | 6.80                         | 1.33                   |
| 0.4                | 46.75               | ---                                     | 5.44                         | 1.06                   |
| 0.3                | 47.00               | ---                                     | 3.92                         | 1.07                   |
| 0.2                | 47.02               |   | 2.87                         | 1.06                   |
| 0.1                | 46.88               | 31.66                                   | 1.29                         | 1.07                   |
| 0.0                | 45.85               | 26.70                                   | ---                          | ---                    |